

Interaction of Visual and Proprioceptive Feedback During Adaptation of Human Reaching Movements

Robert A. Scheidt,^{1,2,3} Michael A. Conditt,^{3,4} Emanuele L. Secco,^{3,5} and Ferdinando A. Mussa-Ivaldi^{2,3}

¹Department of Biomedical Engineering, Marquette University, Milwaukee, Wisconsin; ²Department of Physical Medicine and Rehabilitation, Northwestern University Medical School, Chicago, Illinois; ³Sensory Motor Performance Program, Rehabilitation Institute of Chicago, Chicago, Illinois; ⁴Institute of Orthopaedic Research and Education, Houston, Texas; and ⁵Dipartimento di Informatica e Sistemistica, Università di Pavia, Pavia, Italy

Submitted 3 September 2004; accepted in final form 15 January 2005

Scheidt, Robert A., Michael A. Conditt, Emanuele L. Secco, and Ferdinando A. Mussa-Ivaldi. Interaction of visual and proprioceptive feedback during adaptation of human reaching movements. *J Neurophysiol* 93: 3200–3213, 2005. First published January 19, 2005; doi:10.1152/jn.00947.2004. People tend to make straight and smooth hand movements when reaching for an object. These trajectory features are resistant to perturbation, and both proprioceptive as well as visual feedback may guide the adaptive updating of motor commands enforcing this regularity. How is information from the two senses combined to generate a coherent internal representation of how the arm moves? Here we show that eliminating visual feedback of hand-path deviations from the straight-line reach (constraining visual feedback of motion within a virtual, “visual channel”) prevents compensation of initial direction errors induced by perturbations. Because adaptive reduction in direction errors occurred with proprioception alone, proprioceptive and visual information are not combined in this reaching task using a fixed, linear weighting scheme as reported for static tasks not requiring arm motion. A computer model can explain these findings, assuming that proprioceptive estimates of initial limb posture are used to select motor commands for a desired reach and visual feedback of hand-path errors brings proprioceptive estimates into registration with a visuocentric representation of limb position relative to its target. Simulations demonstrate that initial configuration estimation errors lead to movement direction errors as observed experimentally. Registration improves movement accuracy when veridical visual feedback is provided but is not invoked when hand-path errors are eliminated. However, the visual channel did not exclude adjustment of terminal movement features maximizing hand-path smoothness. Thus visual and proprioceptive feedback may be combined in fundamentally different ways during trajectory control and final position regulation of reaching movements.

INTRODUCTION

Hand-path kinematics are important regulated features of reaching movements with trajectories normally being straight and smooth (Morasso 1981). When an unexpected mechanical perturbation displaces the hand from its intended trajectory, the resulting hand-path errors are rapidly compensated by an adaptive, feed-forward control mechanism (i.e., motor adaptation) (Lackner and Dizio 1994; Shadmehr and Mussa-Ivaldi 1994). Subjects use memories of hand-path errors and perturbation strengths experienced during the most recent movements to improve the straightness and smoothness of movement (Scheidt et al. 2001; Thoroughman and Shadmehr 2000).

This adaptation can occur either with visual feedback or in its absence (i.e., with somatosensory feedback alone) (cf. Dizio and Lackner 1995, 2000; Krakauer et al. 1999; Sainburg et al. 1995; Tong et al. 2002). While vision can partially substitute for proprioceptive feedback when afferent neural pathways are compromised (as in large fiber neuropathy subjects) (Ghez et al. 1995; Sainburg et al. 1995), afferent feedback from limb proprioceptors such as muscle spindles, joint receptors, and, potentially, ligamentous and skin receptors (Prochazka 1996) is sufficient to guide execution of approximately straight and smooth reaching movements. This can occur even in the complete absence of prior visual experience (i.e., in the congenitally blind) (Dizio and Lackner 2000). Because both proprioceptive and visual feedback can be used to compensate for environmental perturbations, it remains unclear exactly how multi-modal sensory information is combined to guide the adaptive updating of motor commands enforcing kinematic regularity of hand path.

There are instances wherein the visual and proprioceptive senses “overlap,” informing the brain about common conditions of the body and its environment. For example, the hand can be localized in space by both vision and proprioception (cf. Graziano 1999; Graziano et al. 2000). Static limb position information from these two senses appears to be combined using a weighted average of the individual signals (Graziano 1999; van Beers 1996), a strategy that may in fact yield optimal statistical properties (cf. Ernst and Banks 2002). However, intrinsic differences in sensor filter characteristics and coordinate reference frames give rise to discrepancies in the information provided to the brain by the different senses, leading to biases and errors in the estimation of limb configuration. Discrepancies may also arise due to variability in sensory transduction and neural encoding processes (i.e., “sensor noise”) (Schreiner et al. 1978; van Beers et al. 2002; Whitsel et al. 1977; see also Cordo et al. 1994) or as a result of neural approximations to the complex nonlinear computations required to map joint angles to fingertip position or vice versa (cf. Flanders et al. 1992; Ghez et al. 1999). One way to resolve sensory conflicts (and to minimize computational requirements) is to allow the senses to compete, with the most reliable sense capturing the multi-modal percept (Gharamani et al. 1997; cf. McDonough and Whalen 1995). In this “competitive” or “winner-take-all” strategy, one sense determines the sub-

Address for reprint requests and other correspondence: R. A. Scheidt, Dept. of Biomedical Engineering, Olin Engineering Center, 303, P.O. Box 1881, Marquette University, Milwaukee, WI 53201-1881 (E-mail: scheidt@ieec.org).

The costs of publication of this article were defrayed in part by the payment of page charges. The article must therefore be hereby marked “advertisement” in accordance with 18 U.S.C. Section 1734 solely to indicate this fact.

ject's behavior while the others are ignored (cf. Rossetti et al. 1995). A competitive strategy is inherently nonlinear because it would not adhere to the principle of superposition required of all linear, time-invariant systems (cf. Ziemer et al. 1983). This contrasts with a cooperative strategy using fixed or slowly adapting weights where superposition would be expected to apply. And while several experimental studies have explored the dominant role of vision during trajectory control (e.g., Flanagan and Rao 1995; Wolpert et al. 1994, 1995), it is yet not clear whether vision and proprioception jointly guide motor adaptation or whether availability of visual feedback precludes the use of proprioception for this purpose.

We performed a series of experiments exploring the integration of visual and proprioceptive estimates of hand-path error during adaptation of reaching movements to a novel dynamic environment. Subjects grasped and moved the handle of an instrumented robot, which pushed the hand away from its intended target. Subjects participated in up to three experimental sessions over a period of several days. Each session challenged them to move in the perturbing field when provided with one of three visual feedback conditions: accurate visual feedback (wherein motion of a cursor on a computer monitor accurately represented the hand's real motion), no visual feedback, and a "false visual feedback" case wherein the cursor represented a projection of the hand's actual trajectory onto the straight line passing from starting to ending target. Implicit in this last case is the possibility that subjects could use unaltered proprioceptive feedback of movement errors to drive adaptive improvements in motor performance. These experiments were designed to test the hypothesis that, like sensory integration for static limb position estimation tasks, sensory integration for the adaptive control of reaching may be described using a weighted sum of performance error information from proprioceptive and visual sources. Testing whether a linear integration model describes subject behavioral data is a way to establish whether movement error estimates derived from the two senses have been effectively normalized to a common coordinate frame. This is a significant question because it probes the computational nature of sensory integration necessary for an important form of motor learning: motor adaptation. Portions of this work were presented at the 1997 and 2003 meetings of the Society for Neuroscience (Conditt et al. 1997b; Secco et al. 2003).

METHODS

Sixteen healthy, right-handed subjects provided written consent to participate in this study with institutional IRB approval. Five subjects participated in a multi-session experimental protocol (*P1*), which comprises the main body of this report, whereas 11 subjects participated in one of two, single-session, supporting protocols (*P2* and *P3*). Subjects executed 0.5-s, 12.0-cm reaches in the horizontal plane while holding the handle of an instrumented, two-joint robot with their dominant arm. This set-up has been described in detail previously (Conditt et al. 1997a). Movements started from the approximate center of the subject's dominant-hand workspace and were made toward eight target locations (1.0-cm square) equally spaced around the periphery of a circle (i.e., movements directions were separated by 45°). Whereas visual presentation of target location was always present, visual feedback of hand position was only sometimes presented via a cursor on a computer monitor mounted directly in front of the subject (main experiments) or via a cursor projected onto a

screen just above the plane of movement (supporting experiments). Direct view of the arm was blocked at all times by an opaque screen. Subjects were asked to reach from the start target to a final target in 0.5 s. No explicit instructions regarding hand path were given. Coarse feedback of movement duration was provided after each trial (too fast: <0.45 s, too slow: >0.55 s, or just right: 0.45–0.55 s). Subjects were instructed to relax after each movement while the robot moved the hand slowly back to its starting position. No visual feedback of hand position was provided during the robot-assisted return movement.

The robot's motors generated torques canceling the passive inertia of the robot's linkages and motor shafts during each trial (the "null environment") (Conditt 1998; Conditt et al. 1997a). In the main protocol *P1*, the robot also pushed the hand on some trials with forces proportional and perpendicular to the hand's instantaneous velocity (a counter-clockwise, viscous curl field; Eq. 1; Fig. 1A)

$$\begin{bmatrix} F_x \\ F_y \end{bmatrix} = \begin{bmatrix} 0 & -13 \\ 13 & 0 \end{bmatrix} \begin{bmatrix} \dot{x} \\ \dot{y} \end{bmatrix} \quad (1)$$

where \dot{x} and \dot{y} were the components of the hand velocity along the left/right (x) and proximal/distal (y) directions. F_x and F_y were the components of the force applied along the same directions.

Experimental protocol

Subjects in protocol *P1* participated in three experimental sessions over a period of several days, each session characterizing adaptation in one of three visual feedback conditions (Fig. 1B). Sessions were randomly presented to minimize order dependencies. In the VP case (consistent visual and proprioceptive feedback), a cursor representing the hand's position was presented on the computer screen according to a linear mapping from hand coordinates to screen coordinates. In the "proprioception only" P case (no ongoing visual feedback), subjects were provided with visual feedback of hand position only at the start position prior to each movement but not after the cursor left the initial target region (i.e., visual feedback of trajectory is lacking altogether when vision is blocked during movement). In the "visual channel" V_{chan} case, the cursor was a projection of the actual hand trajectory onto the straight line passing from starting to end target. This orthogonal projection eliminated hand-path direction errors and allowed us to test whether subjects would use proprioceptive feedback, which was unaltered, to drive compensation for directional errors. Subjects had the visual perception that they were performing straight-line hand movements regardless of deviations from that ideal path. In all three experimental conditions, full and accurate feedback of hand position was presented while the hand was at the starting target (i.e., until the hand speed exceeded 0.1 m/s) after which one of the three feedback conditions described in the preceding text was applied.

It is important to note that the orthogonal projection has a desirable property not provided by simple rotations of the visual coordinate frame about the home target: the visual channel creates redundancy in the mapping of hand motion onto cursor motion such that adaptive corrections for direction errors are not absolutely required to bring the cursor to the target. When a perturbation or other change in operating condition induces direction errors, subjects can adjust movement extent alone, or they can correct both direction and extent. In the absence of experimentally induced errors, the visual channel by construction allows subjects to persist in making smooth movements straight to the intended target. It also allows nonstationarity in motor planning to be expressed in the gradual evolution of direction errors (at the cost of requiring hypermetric movements). Nonstationarity could result from optimizations intrinsic to motor planning/control as well as from inherent adaptations in the sensory transduction of limb kinematics. Thus the orthogonal projection provides a novel means of exploring how proprioception (which was unaffected by the projection) and vision may differentially contribute to the planning and adaptation of goal-directed reaching.

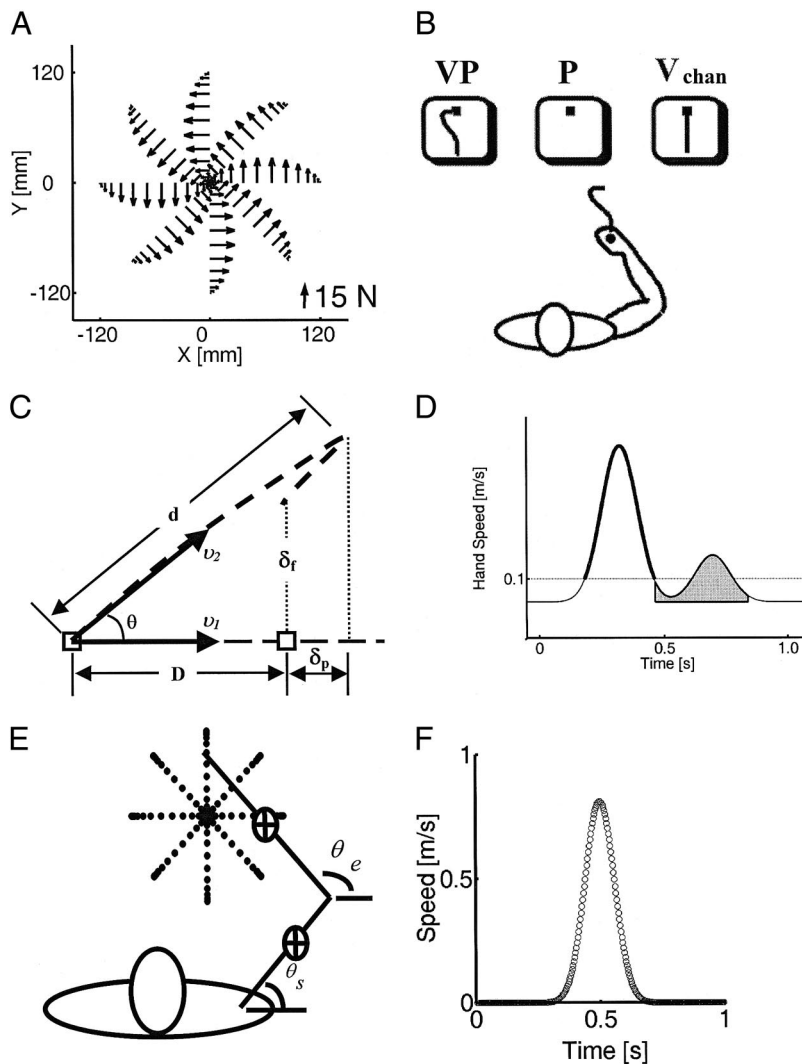


FIG. 1. Hand forces (A) were experienced on certain trials while subjects were provided with 1 of 3 visual feedback conditions (B) on separate days. When provided with concurrent visual and proprioceptive feedback (VP condition), subjects could see a cursor that accurately represented the location of their hand during movement. In the “proprioception only” (P) condition, subjects only saw their hand location while the cursor was in the initial starting position. In the visual channel (V_{chan}) condition, subjects could see a cursor during movement, but the cursor did not accurately represent the hand’s location in space. Rather the cursor was a projection of the actual hand trajectory onto the straight line passing from starting to end target. No visual feedback of hand position was provided during the robot-assisted return to the starting target. C: schematic representation of kinematic performance measures used to evaluate subject performance during the reaching task. Initial and final targets (squares) were separated by a distance $D = 12.0$ cm in the horizontal plane of the robot. In some instances, subjects made initial direction errors, θ , calculated as the interior angle between 2 vectors: the first v_1 , passing through the initial and final targets while the second v_2 was directed from the initial target toward the point in the hand’s trajectory (thick dashed line) when the hand speed reached its transient maximum. Peak movement extent, d , was calculated as the hand’s maximum travel from the initial target. Task-relevant extent error, δ_p , (extent error in projection along the straight line path between initial and final target) was calculated by calculating the difference between the orthogonal projection of d onto the v_i and the desired movement distance D . Final position error, δ_r , was calculated as the Euclidean distance between the hand’s final position following movement and the desired target location. D: schematic representation of a hand-speed profile used to demonstrate the calculation of the hand-speed asymmetry index. In this example, hand speed has a fast primary movement and a slower secondary submovement. Onset of the primary movement is taken as the point in time when the hand speed first exceeds 0.1 m/s. An ideally symmetric primary movement (thick solid line) was constructed by appending to the initial speed profile (from movement onset to peak hand speed) a reflected version of itself. A hand-speed asymmetry index (shaded area) was calculated as the integral of the actual hand-speed profile over the time period beginning when the idealized hand-speed profile dropped below 0.1 m/s and ending 0.40 s later. E: lumped-parameter arm model used to predict hand paths via forward dynamic simulations as presented in the APPENDIX. F: the bell-shaped tangential hand-speed profile used to estimate the joint torques required to move the arm model through the hand paths as depicted in E.

Each session consisted of five blocks of 192 trials separated by ~2–3 min of rest during which subjects were instructed to relax and remain still. Each block consisted of 24 “cycles” of eight movements directed toward each of eight targets equally spaced about the perimeter of a circle of 12 cm radius. The order of target presentation was pseudorandomly distributed within each cycle. The first block of movements consisted of *baseline* trials that were made in the null environment. The viscous curl field was added pseudorandomly once every eight trials. Such “curl-field catch trials” were used to assess the subject’s initial response to the field before onset of adaptation. Catch trials were embedded within the movement cycles such that each of the eight catch trial directions was sampled once every eight cycles (i.e., a super-cycle). Cursor feedback was provided at all times in the VP and V_{chan} cases, even during catch trials. Three blocks of *adaptation* trials followed, during which the manipulandum presented the curl field on seven of eight trials. Occasionally, the curl field was removed to assess progress of adaptation, as indicated by the presence of aftereffects. These “null-field catch trials” occurred with the same frequency and super-cycle structure as the curl-field catch trials. Finally, a block entirely composed of null-field movements was performed (i.e., no curl field applied; *recovery* trials). Experimental sessions lasted ~2.5 h each.

Two supporting, single-session experiments were performed to elucidate how repeated exposure to the null-field environment (P2) and exposure to oppositely directed (clock-wise) force-field perturba-

tions (P3) within the visual channel might contribute to the evolution of hand-path errors as will be described for *protocol P1*. In both P2 and P3, subjects were required to sit for one session that was equivalent to the V_{chan} session of P1. In *protocol P2*, however, no additional perturbing forces (Eq. 1) were applied during the “adaptation” blocks. Subjects were simply asked to move over and over again in the null field while provided with orthogonally-projected visual feedback. In *protocol P3*, the sign of the perturbations of Eq. 1 was inverted, providing subjects with exposure to clockwise viscous curl force perturbations. In an attempt to keep the experimental session within a more manageable time frame (~1.5 h), the number of targets in *protocol P3* was reduced to three (from 8) and the in-field training period was truncated somewhat: subjects performed one block of 240 movements with full exposure to the perturbations (no catch trials) and one block of 300 movements which included 264 curl field trials and 32 null field trials. No recovery trials were performed in *protocol P3*.

Data analysis

Task performance was quantified using several measures that evaluated different aspects of hand-path kinematics. First, we defined *hand-path error* as the integrated deviation from the ideal, straight-line path between initial and final targets over the 0.5-s duration of movement to evaluate how well subjects were able to make directed

movements. This measure of performance makes the assumption that subjects intended to make straight-line reaching movements in the absence of explicit instructions regarding hand path (Atkeson and Hollerbach 1985; Morasso 1981). Movements to the subject's right and parallel to the frontal plane were considered 0° movements.

We decomposed overall hand-path error into errors of extent and direction (Bock and Arnold 1993; Gordon et al. 1994; Rosenbaum 1980; Sainburg et al. 2003; see also Ghez et al. 1993, 1999). Peak movement extent in each trial was calculated as the transient maximum deviation from the initial target (d in Fig. 1C). Movements with substantial "overshoot" would have greater movement extent values than those that failed to reach all the way to the target. *Extent error* was simply the difference between movement extent and the desired movement extent ($D = 12$ cm in Fig. 1C). Movement extent error in projection along the straight-line path between initial and final target (i.e., cursor movement in the V_{chan} case) was also calculated, but instead of considering the entire trajectory, only the component contributing to motion along the desired trajectory was used in the computation (δ_p in Fig. 1C). This projection corresponds to the cursor movement as seen by subjects during the V_{chan} feedback condition. *Direction error* was calculated as the angular difference between two vectors: the first was drawn between initial and desired final targets, whereas the second was drawn between the initial target and the point in the hand's true trajectory when the hand speed reached its transient maximum. We also computed *final position error* as the magnitude of error between final hand position and the desired target location (δ_f in Fig. 1C). This measure evaluated how well subjects were able to acquire the final target.

Baseline hand trajectories were generally smooth with approximately symmetric, bell-shaped hand-speed profiles. We sought to determine how the symmetry of hand-speed profiles might be perturbed on initial exposure to the viscous curl force field and whether or not symmetry would be recovered with repeated exposure. But because perturbed hand-speed profiles are not always symmetric about the peak and sometimes exhibit secondary peaks (consistent with the presence of corrective submovements), we computed a *hand-speed asymmetry* index as an estimate of skewness in the speed profile. We did this by first constructing an idealized, symmetrical hand-speed profile for each trial by appending to the initial speed profile (from movement onset to peak hand speed) a reflected version of itself. We then computed the asymmetry index by integrating the actual hand-speed profile for 0.40 s starting from when the idealized hand-speed profile dropped below a threshold value of 0.1 m/s (Fig. 1D). The magnitude of this index was near zero when the trajectory was symmetric. Its magnitude grew with the size and number of additional peaks and with skewness of hand speed.

We evaluated the time course of changes in these performance measures by calculating the *majority* and *catch trial* performance averages within movement cycles. Specifically, the majority average (of 7 movements) was taken as the mean across all non-catch trials within a given cycle of eight movements. The catch trial cycle average was taken as the mean across all catch trials within a super-cycle of eight catch trials. We evaluated overall changes in average performance across subjects by computing the percentage change in hand-path error during each experimental stage ($\% \Delta E$). This measure was calculated by normalizing each subject's block-average performance by the initial exposure errors collected at baseline: $\% \Delta E = 100[(E_i/E_{\text{baseline}}) - 1]$, where E_i is the hand-path error averaged within each block i of trials, and E_{baseline} is the hand-path error averaged within the baseline block of trials. ANOVA and post hoc tests were used to compare percentage change in hand-path error across sensory feedback conditions at the end of adaptation. Similarly, we normalized each subject's average hand-speed asymmetry values by the unperturbed baseline average to obtain percentage change in hand-speed asymmetry as a function of increasing exposure to the perturbation: $\% \Delta \text{Asymmetry} = 100[(A_i/A_{\text{baseline}}) - 1]$, where A_i is the average

asymmetry value for each block i , while A_{baseline} is the average asymmetry value calculated for the baseline block.

Computer simulations

Subjects frequently err in estimating limb configuration when they are required to compute hand position without view of their hand (Brown et al. 2003; van Beers et al. 1999; Wann and Ibrahim 1993). They also make directional errors or biases when reaching without view of their hand (Ghilardi et al. 1995; Vindras et al. 1998). These biases have been explained as arising from drift of the representation of either hand or target location toward the workspace location in which motor tasks are most frequently performed (Ghilardi et al. 1995; Wann and Ibrahim 1993). We performed a set of forward dynamic numerical simulations similar to those described by Brown et al. (2003) to evaluate the consequence of misestimating initial limb posture on the subsequent generation of reaching movements (cf. Desmurget et al. 1998) and to determine whether errors in position estimation could explain performance in the V_{chan} case. The simulations assumed that subjects did *not* adapt their initial motor commands to the force-field perturbation when visual feedback of hand-path errors perpendicular to the intended movement was eliminated.

First a set of eight template movements in the horizontal plane were created, starting from an initial limb configuration in the approximate center of an "average" subject's right-hand workspace and ending at eight equally spaced targets along the periphery of a circle with 12 cm radius (Fig. 1E). These straight-line movements had bell-shaped hand-speed profiles (Fig. 1F). Limb segment lengths and other mechanical properties for this average subject were taken from literature describing previous simulations of reaching and adaptation to perturbing force fields (Shadmehr and Mussa-Ivaldi 1994). Next, inverse kinematic and inverse dynamic calculations were performed to estimate joint torques needed to drive the simulated limb through desired hand paths (see APPENDIX). In addition to the feed-forward torques calculated about the nominal "desired" movements, the limb also generated restoring forces about the desired trajectory due to the effective viscoelastic properties of muscle and passive tissues. These forces supplement the feed-forward torques calculated about the nominal trajectories when the hand deviated from that path. The desired movements are represented as time series of joint angle changes relative to the initial limb configuration. We then evaluated the sensitivity of unperturbed hand-path kinematics to errors in estimating the limb's initial configuration. We did this by recalculating the template movements and feed-forward joint torques starting from another, different region of the workspace. These recalculated joint torques and joint angle equilibrium trajectories were then applied starting from the limb's original initial configuration to simulate errors in movement planning arising from misestimation of the limb's initial configuration. No additional perturbing forces were simulated as we were attempting to model performance in the null-field after repeated exposure to the viscous curl force field (i.e., Fig. 2C, 4th panel). We used the simplex method (a multidimensional, unconstrained, nonlinear, optimization technique) (cf. Lagarias et al. 1998; Press et al. 1988) to select the hand's initial $\{x,y\}$ location that minimized the difference between simulated and the average subject direction errors and peak extent errors. Finally, we validated these efforts by simulating motions performed in the presence of the viscous curl field and starting from $\{x,y\}$, but using the motor program inferred from the original null-field movements.

RESULTS

Average hand paths made by a representative subject before, during, and after extended exposure to a viscous curl force field in *protocol P1* (Fig. 2) display features common to all subjects tested. When provided with concurrent visual and propriocep-

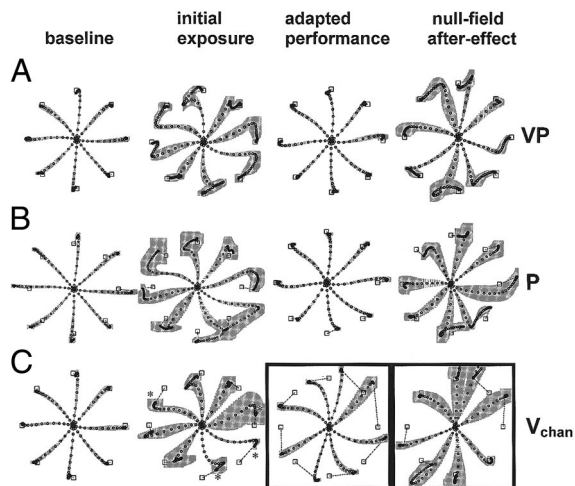


FIG. 2. Hand paths generated by a representative subject. A: VP; B: P; C: V_{chan} . *1st column*: average hand paths from null-field movements in the baseline block of trials (i.e., movements with the motors cancelling the robot's passive dynamics, but with no additional force field added). *2nd column*: average hand paths from occasional perturbed movements in the baseline block. The field applied was a viscous curl-field (Eq. 1). *3rd column*: average hand paths from perturbed movements in the final adaptation block of trials. *4th column*: average hand paths from occasional unperturbed movements in the final adaptation block. Shading indicates 95% confidence interval (CI) of the trajectories in the x and y directions. Asterisks in the 2nd panel of C indicate directions wherein movements had "hooks" that were nearly perpendicular to the visual constraint. The set of movements highlighted within the boxes are the primary focus of the simulations described in the text.

tive feedback (VP condition), subjects performed as in previous studies of adaptation to viscous force-field perturbations (cf. Shadmehr and Mussa-Ivaldi 1994): hand paths that had been straight and smooth (Fig. 2A, *1st panel*) deviated dramatically from ideal straight line movements on initial exposure to a perturbing force field (*2nd panel*), often with characteristic "hooks" near the end of movement. After repeated exposure to the field, the subject learned to eliminate directional errors induced by the perturbations. They also eliminated terminal features (secondary submovements) inconsistent with a stereotypical smooth, bell-shaped velocity profile (*3rd panel*). Unexpectedly removing the perturbation caused well-formed aftereffects that were approximately mirror-symmetric to the initial exposure errors (*4th panel*). Well-formed aftereffects reflect the presence of an internal model of the dynamics of the limb and its environment (Shadmehr and Mussa-Ivaldi 1994).

Proprioception suffices to guide recovery of movement direction after perturbation

Similar performance was observed when subjects reached without ongoing cursor feedback (i.e., with proprioceptive feedback alone, P; Fig. 2B). As in the VP case, hand paths that had been straight and smooth (Fig. 2B, *1st panel*) deviated from straight-line movements on initial exposure to the perturbation (*2nd panel*) with "hooks" near movement end. Subjects learned to eliminate directional errors and terminal hooks after repeated exposure to the field (*3rd panel*). While hand paths were smooth and directed straight to the target, movement extent was less well regulated (data shown in the following text). Aftereffects observed when the perturbation was unexpectedly removed (*4th panel*) reveal that proprioceptive feedback indeed sufficed for learning novel environment dynamics.

This is consistent with previous reports that proprioception suffices to guide internal model formation during reaching (Krakauer et al. 1999; Tong et al. 2002) in the congenitally blind (Dizio and Lackner 2000).

Eliminating visual feedback of perpendicular hand-path errors disrupts adaptive responses

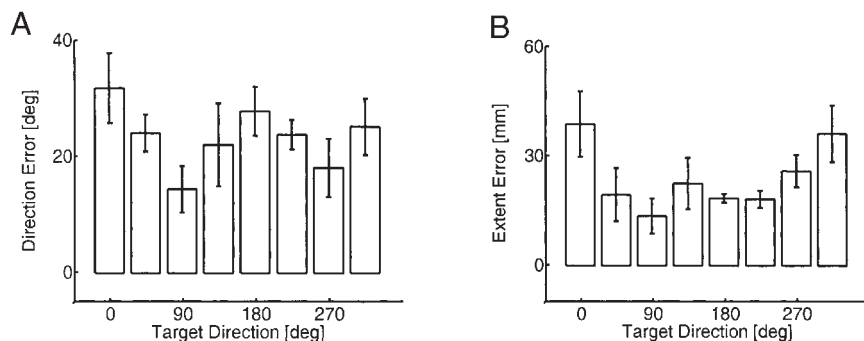
In contrast to the VP and P conditions, presenting visual feedback only in projection along the line connecting starting and end targets (Fig. 2C) significantly impaired correction of initial direction errors during reaching (*2nd panel*). In fact, these errors increased with repeated exposure to the field (*3rd panel*). The hand frequently stopped far from its objective, even after 400 repeated attempts to move in the field (the dashed lines from movement endpoint to final target indicate which target the subject was asked to move to). Note that some of the movements were initially directed up to 45° from the target. These errors occurred even though subjects generally were capable of making smooth movements as revealed by the suppression of terminal "hooks" or "submovements" (*3rd panel*). We observed consistent behavior across subjects. Direction and extent errors varied significantly with target direction in the presence of the force field (Fig. 3, A and B, respectively): reaches toward all targets were deflected in the direction of the perturbing force field and tended to be hypermetric. Interestingly, direction errors persisted in movements toward some targets on removing the field (albeit to a lesser extent than in the perturbed trials) while extent errors (with hooks) were dominant in movements to other targets (Fig. 2C, *4th panel*). We observed consistent behavior across subjects: direction and extent errors varied significantly with target direction in the null-field following training in the V_{chan} feedback condition (Fig. 3, C and D). Both types of error varied as bimodal functions of target direction.

Assuming that subjects used a common movement strategy in all three feedback conditions, these last findings support the conclusion that the principle of superposition for linear, time-invariant, additive models of sensory integration does not apply in the case of the adaptive trajectory regulation during reaching. Subjects clearly were capable of using proprioceptive information alone to correct errors in movement directions induced by the curl field, yet they failed to do so when visual feedback of perpendicular hand-path errors was eliminated. Subjects also consistently made catch trial errors in the direction of the perturbing force field after V_{chan} training. Even if proprioceptive error information was partially (incompletely) attenuated, then we would have expected in-field errors to decrease (not increase) with practice, and we would have expected catch trial errors to be directed opposite to (not along) the curl-field perturbation direction. Because neither expectation was met, the additive model of sensory integration can be rejected. Anecdotally, no subject reported being aware of the visual channel manipulation when asked to describe his/her experience after that session.

Evolution of performance changes with repeated force-field exposure

Reduction in performance error to some original baseline level despite persistent perturbation is a hallmark of motor

V_{chan} in-field errors



V_{chan} catch-trial errors

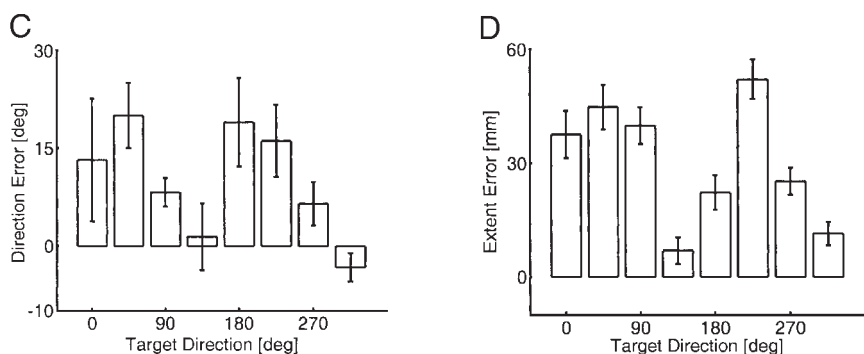


FIG. 3. Initial direction (A) and extent (B) errors as a function of target direction averaged across subjects during viscous perturbation in the V_{chan} condition. Error bars represent 95% CI of the mean. Direction (C) and extent (D) errors without mechanical perturbation (i.e., the null field) in the V_{chan} condition.

adaptation. We evaluated the presence and evolution of motor adaptation by plotting the cycle-averaged, integrated hand-path errors (both majority and catch-trial) as a function of cycle number for the three visual feedback conditions. This representative subject's in-field hand-path errors (Fig. 4, top row) were rapidly eliminated after onset of persistent field exposure—within one or two movement cycles (filled circles, VP and P conditions). Eliminating the perturbation during the adaptation in these two feedback conditions evoked oppositely directed hand-path errors consistent with the formation of an internal representation of the force-field perturbation (Shadmehr and Mussa-Ivaldi 1994). Removing perturbation altogether caused the subject to rapidly reacquire baseline performance in the recovery block of trials. These results contrast with performance in the V_{chan} feedback condition. Here, repeated exposure to the viscous curl force field caused both in-field and catch-trial hand-path errors to increase progressively in the direction of the perturbation. Interestingly, when the persistent perturbation was turned off (i.e., during recovery), the subject persisted in making movements that had considerable hand-path errors in the same direction as the in-field errors. All five subjects exhibited the same behavior. ANOVA (Minitab 13; Minitab) performed on the final block of force-field trials showed that integrated hand-path errors made after 400 trials in the viscous field depended strongly on the type of error feedback provided [$F(2,12) = 34.8, P < 0.0005$]. A post hoc, two-sample *t*-test reveals no significant differences in the mean errors made in the VP and the P conditions ($T = 0.67, P = 0.54$). Accordingly, these data were pooled in another post hoc, two-sample *t*-test revealing a significant increase in movement errors made in the V_{chan} condition when compared with the VP and the P conditions ($T = 6.9, P =$

0.001). Subject performance degraded in perturbation trials wherein hand-path error information was artificially minimized in the visual feedback. Clearly, eliminating visual feedback of hand-path deviations from a straight-line reach compromised motor adaptation.

We decomposed the overall hand-path errors into errors of initial movement direction and of peak movement extent (Fig. 4, 2nd and 3rd rows, respectively). Changes in initial direction error paralleled those observed for hand-path errors, with error reduction and aftereffects consistent with motor adaptation in the VP and P cases. In-field and catch trial errors increased progressively in the V_{chan} case. Consistent patterns of initial direction error performance were observed across subjects. Subjects eliminated directional errors after repeated exposure to the field in the P case, (mean in-field error in the final perturbation block was not different from 0: one-sample *t*-test: $T = 2.02, P = 0.11$). Significant aftereffects of adaptation were observed at the end of training ($T = -3.70, P = 0.021$) demonstrating that reduction of directional errors observed in perturbed trials was not simply due to stiffening the limb but rather to a feed-forward compensatory mechanism that does not require visual feedback of ongoing movement. For the V_{chan} case, both in-field hand paths and unperturbed catch-trial movements increasingly deviated from their intended target direction with repeated exposure to the field. Across subjects, there was a statistically significant increase in error from the first block of trials to the last [$F(5,49) = 2.86, P = 0.024$]. And as expected, direction errors were greater when the field was on than when the field was off [$F(1,53) = 59.6, P < 0.0005$].

Peak hand-path extent errors exhibited a somewhat different pattern of behavior, as can be seen in row 3 of Fig. 4. While both perturbed and unperturbed movements were of the correct

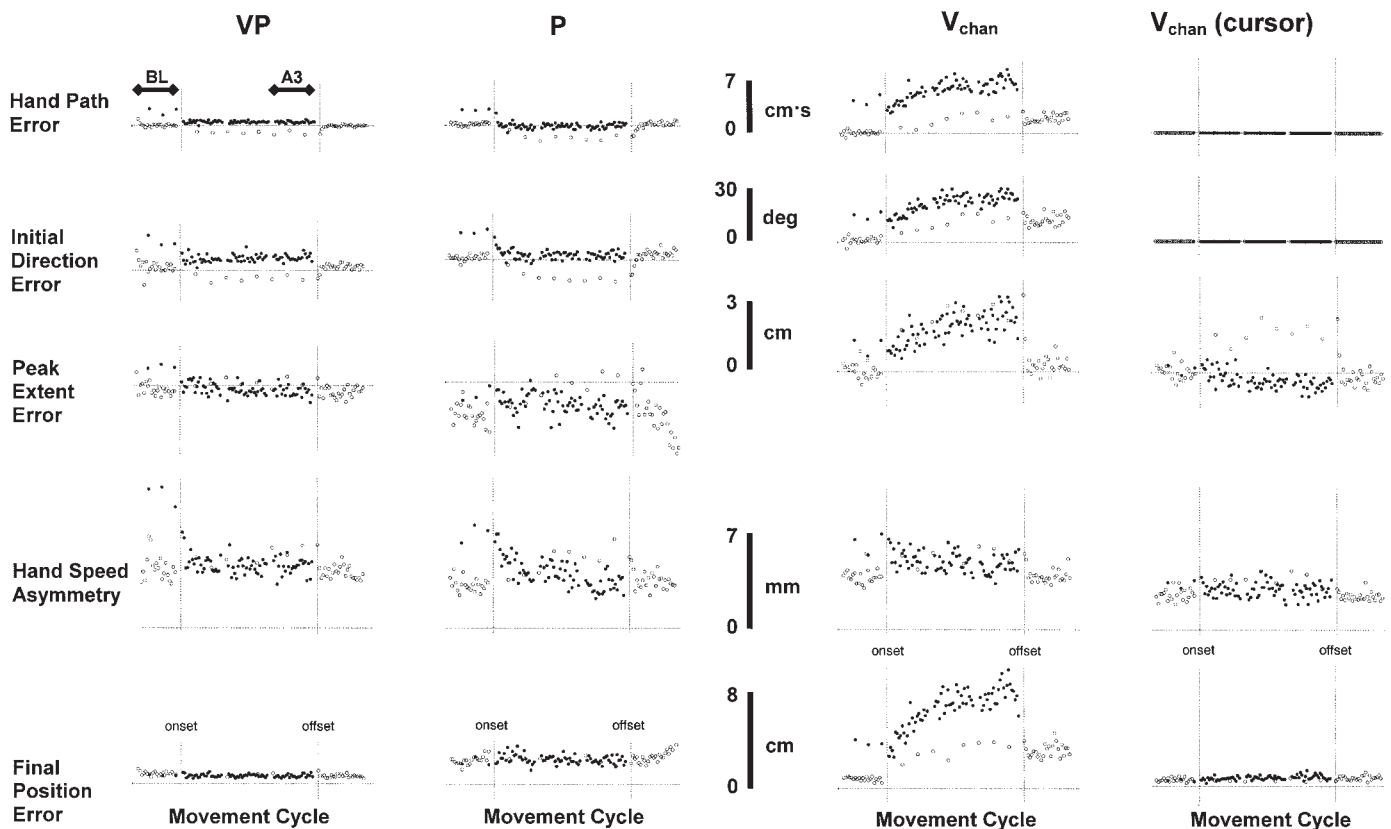


FIG. 4. Evolution of kinematic performance changes as a function of movement cycle presentation order before, during, and after prolonged exposure to a viscous curl force-field perturbation during reaching for a single, representative subject. Five kinematic performance measures are presented: integrated hand-path error (*top row*), initial direction error (*2nd row*), peak extent error (*middle row*), hand-speed asymmetry index (*4th row*), and final hand position error (*bottom row*). Three columns present plots of hand kinematic performance for each of the 3 visual feedback treatments: veridical visual and proprioceptive feedback (VP), no ongoing visual feedback during movement (i.e., proprioception alone, P), and the visual channel condition (V_{chan}); please see text for a detailed description of this treatment). *4th column*: plots of *cursor* kinematic performance in the V_{chan} feedback condition. Vertical lines indicate the onset and offset of adaptation phase training. Filled symbols indicate movement cycle averages of in-field performance measures. Open symbols indicate movement cycle averages of null-field performance measures. The thick bars at the top of the VP column indicate the baseline (BL) and last “adaptation phase” (A3) blocks. Most statistical comparisons presented in the text evaluated differences in performance between the BL and A3 trial blocks.

extent in the VP case, movement distance was not well regulated in the P case. Whereas ANOVA revealed no significant pattern of extent errors as a function of perturbation type (i.e., field or no field) or of block number, analysis of errors made by individual subjects reveals substantial diversity in the pattern of extent errors, both as a function of block number as well as between the perturbation conditions. In the unperturbed trials, one subject *increased* movement extent *toward* the ideal 12-cm movement length, one subject *decreased* movement extent *away* from the ideal, two subjects *decreased* extent *toward* the ideal, and the last subject first *increased* away from then *decreased* extent *toward* the ideal. Similar diversity was observed in the perturbed trials. Two subjects *decreased* movement extent *away* from the ideal with repeated exposure to the field, two more *decreased* extent *toward* the ideal, and again, the last subject first *increased*, then *decreased* movement extent. Over the entire training period, and considered across subjects, these average extent errors ranged from -6 to $+8$ cm. This variability implies that movement extent is not well regulated without ongoing visual feedback of movement performance.

Peak extent errors of hand movement in the V_{chan} condition reflect the constraint imposed by the orthogonal transformation

implementing the visual channel. When peak extent errors are viewed in projection (i.e., when we consider motion of the cursor and not the hand), in-field errors are quite small, demonstrating that subjects indeed satisfy the task’s visual objectives. They do so, however, by making hand movements that are dramatically hypermetric [as can be seen in both majority and catch-trial averages of overall extent errors (V_{chan}) as well as when catch trials errors are viewed in projection: V_{chan} (cursor)]. This hypermetria is a consequence of increasing movement direction errors (Fig. 4, *2nd row*) and of the orthogonal projection implementing the visual channel. Increasing extent errors were observed in both perturbed and unperturbed trials during training. Averaging across subjects, we observe that hand movements made in the field were always longer than desired, with extent errors at the end of training significantly greater than those at the beginning of training (paired *t*-test: $T = 7.29$, $P < 0.0005$). This was true regardless of whether perturbing forces were active or not. When both movement direction and extent errors are considered, only unperturbed movements in the V_{chan} baseline block were directed accurately at the target with proper extent.

Next, we examined terminal features of movement such as hand-path smoothness and the possible presence of corrective

submovements by quantifying the degree to which hand-speed profiles deviated from the symmetrical, bell-shaped ideal during exposure to the viscous curl force field (Fig. 4, 4th row). Initial null-field movements were quite smooth with few or no secondary peaks in the speed profiles while initial movements in the force field often had several late peaks consistent with the presence of submovements (Fig. 5) (cf. Meyer et al. 1988). Consequently, the hand-speed asymmetry index was elevated on initial exposure to the curl field across all feedback conditions (*t*-test of mean difference = 0: $T = -9.12$, $P < 0.0005$). With repeated exposure to the perturbation, the magnitude and number of secondary peaks in hand speed systematically decreased across all feedback conditions. Across subjects, the average reduction in asymmetry was greatest in the P condition, with the difference between the P and the V_{chan} conditions reaching statistical significance (Tukey's *t*-test: $P = 0.028$). These results indicate that visual feedback of ongoing movement performance is not necessary for reduction of secondary submovements and/or an increase in terminal trajectory smoothness during goal-directed reaching movements.

Last, we evaluated terminal hand position errors (Fig. 4, bottom row), which were observed to be well regulated only when visual feedback of task-relevant performance was available. VP in-field and catch trial movements both had modest terminal position errors: 0.8 ± 0.2 cm (SD) and 0.9 ± 0.3 cm, respectively. When no ongoing visual feedback was provided (P), extended exposure to the perturbation evoked 3.3 ± 2.0 cm and 3.4 ± 1.9 cm final position errors (catch-trial and in-field performance, respectively). Performance was also poor in the V_{chan} case where terminal position errors averaged 7.1 ± 1.7 cm during catch-trial and 2.6 ± 0.3 cm during in-field trials. However, V_{chan} terminal errors were small in projection onto the straight line between initial and final targets—averaging 0.6 ± 0.2 cm during null-field catch-trials and 0.7 ± 0.2 cm during perturbation. Thus reduction of terminal position errors is highly dependent on visual feedback of ongoing movement. When error reduction occurs, it takes place along the spatial dimension for which visual feedback is provided.

Initial direction errors develop spontaneously in the visual channel condition

As demonstrated by the movement cycle averaged direction errors from a representative subject (Fig. 6A), the results from supporting *experiment P2* clearly demonstrate that the development of initial null-field direction movement errors observed in *protocol P1* was not contingent on the presence of the viscous curl force perturbations of *Eq. 1*. While *P2* subjects had to generate small hand forces to overcome the compensated dynamics of the robot (averaging $3.6 + 1.2$ N), these hand forces were just 12% of those experienced by *P1* and *P3* subjects during perturbation trials ($30.7 + 2.1$ N). The increase in direction error during *P2* training ($5.1 \pm 0.3^\circ$; Fig. 6C, thin dashed line) averaged more than half of that for *P1* subjects (57% of $8.9 \pm 0.8^\circ$; Fig. 6C, thick solid line).

Movement cycle averaged direction errors from a typical *P3* subject reveal that a counter-rotating force field elicits movement direction errors in the same direction as those observed in *protocol P1* (Fig. 6B). While these null-field errors are clearly in the direction opposite to the imposed force field, they are not what we would consider typical aftereffects of adaptation because there is no clear indication that subjects attempted to reduce the induced direction errors even after considerable practice (Fig. 6B, dark symbols). Finally, we found no evidence for a difference in the rate at which direction errors developed across protocols [$F(2,13) = 1.1$, $P = 0.36$; Fig. 6C].

Initial direction errors arise from misestimation of initial limb configuration

Knowledge of initial arm configuration is necessary to select appropriate feed forward motor commands for generating reaching movements (Bock and Arnold 1993; Desmurget et al. 1997, 1998; Ghilardi et al. 1995; Rossetti et al. 1995; Sainburg et al. 2003; Sober and Sabes 2003). It has been suggested that the kinematic plan for movement is “formed by combining the visually derived representation of intended final arm orientations with a ‘kinesthetically derived’ representation of initial arm orientations” (Flanders et al. 1992; p. 312). We performed a set of forward dynamic numerical simulations (APPENDIX) to evaluate the consequence of proprioceptive misestimation of the limb’s initial posture on the subsequent generation of

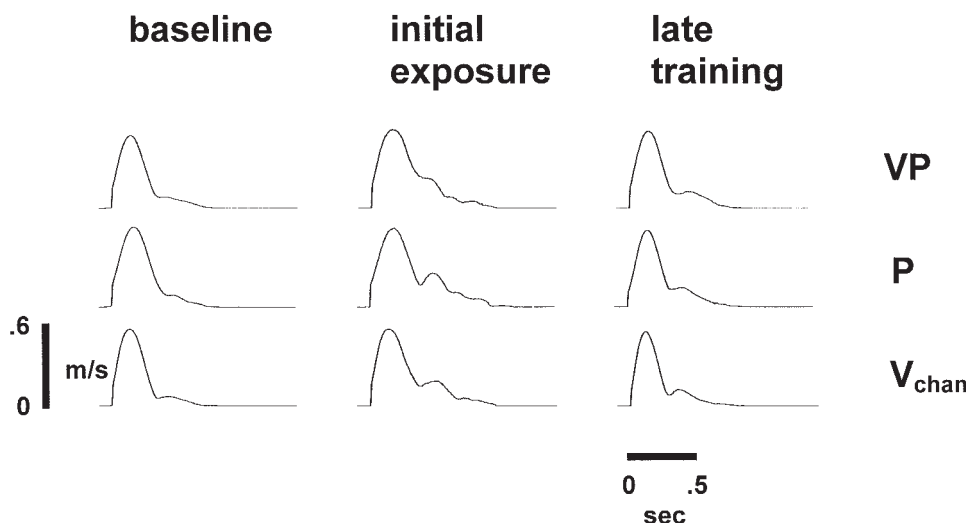


FIG. 5. Sample hand-speed profiles from a typical subject as performed in the null field (left), upon exposure to the viscous curl force field (middle) and after extended training in the field (right) for each of the three visual feedback conditions: VP (top), P (middle) and V_{chan} (bottom).

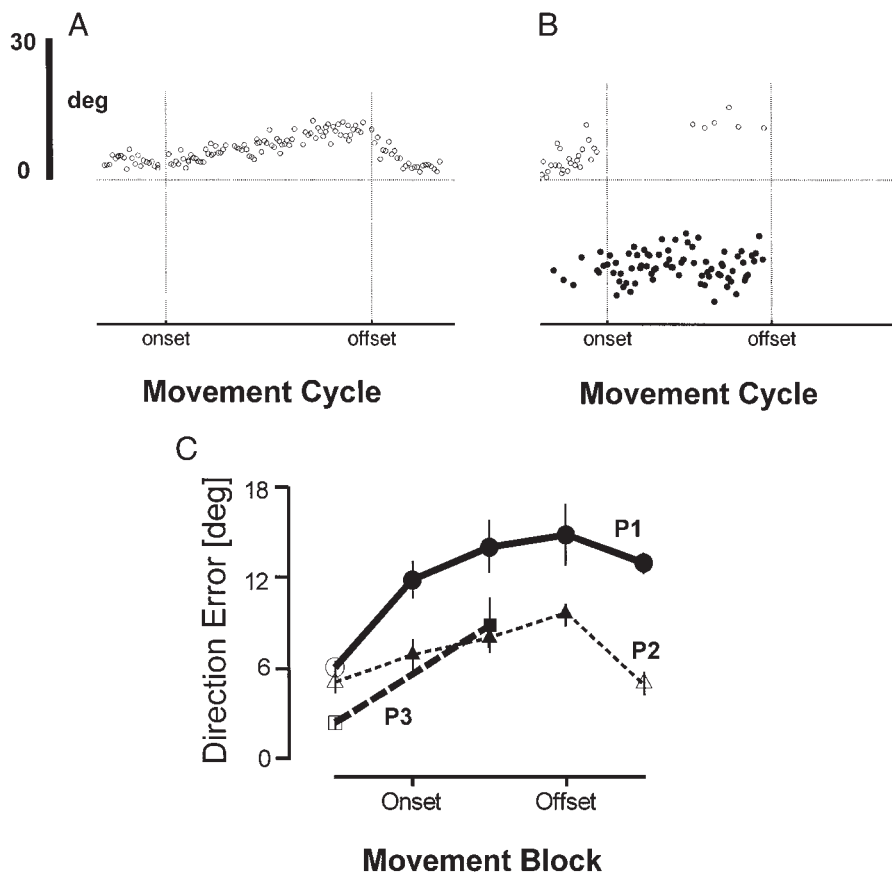


FIG. 6. Analysis of direction errors in supporting experiments P2 and P3. *A*: evolution of direction errors as a function of movement cycle for null-field movements performed by a representative P2 subject. Vertical lines represent the onset and offset of exposure to the visual channel. *B*: evolution of direction errors as a function of movement cycle for clockwise curl-field movements performed by a representative P3 subject. Vertical lines represent the onset and offset of force-field training. *C*: comparison of direction errors as a function of movement block for all 3 subject groups: P1, thick solid line; P2, thin dashed line; P3, thick dashed line. Error bars represent 95% confidence intervals.

reaching movements (cf. Brown et al. 2003; Ghilardi et al. 1995; Sober and Sabes 2003; Vindras et al. 1998; Wann and Ibrahim 1993; but see also Desmurget et al. 2000).

After constructing a set of shoulder and elbow joint torque profiles appropriate to drive the simulated limb through straight line movements in eight different directions, we explored the effect of altering limb initial configuration on hand-path accuracy (i.e., initial direction errors) under feedforward playback of the previously-calculated joint torques (Fig. 7a). Specifically, we optimized selection of two parameters $\{\Delta x, \Delta y\}$ specifying the shift in initial limb configuration that minimizes the mean, squared difference between simulated movement direction errors and the average null-field errors made by subjects in the last adaptation block of P1 V_{chan} trials (Fig. 7B). Next, we evaluated how well the model predicts initial direction errors in the presence of the perturbing viscous curl force field consequent to the identical shift in initial limb configuration (Fig. 7C).

The simulations demonstrate that errors in estimating initial limb configuration (corresponding to errors in shoulder and elbow angle estimation of -5.2 and 28.0° , respectively) can account for initial movement direction errors made in 7 of 8 null-field target directions (the optimization dataset), with the model underestimating subjects' errors very slightly in the remaining direction (Fig. 7B; 315° target direction). The same initial configuration estimation errors also account for direction errors made in the presence of the perturbing force field (the validation dataset) for the same seven target directions with the model again underestimating subjects' errors in the remaining direction (Fig. 7C). The joint angular estimation errors found by our optimization correspond to a displacement of the hand

6.8 cm toward the subject's midline and 13.6 cm toward the subject's chest.

DISCUSSION

These experiments investigated the ability of able-bodied subjects to adapt reaching movements to a novel force field under three different visual feedback conditions: 1) veridical visual feedback that matched cursor movement on a screen to hand position throughout movement, 2) no visual feedback during movement, and 3) false visual feedback wherein cursor feedback of deviations from the straight-line reach were eliminated. We found that when visual feedback of movement is eliminated entirely, proprioception suffices to guide adaptive recovery of straight and smooth hand trajectories directed toward the final target. However, eliminating visual feedback of just the orthogonal hand-path errors did not lead to reduced direction errors. Instead, hand-path errors were observed to *increase* with repeated exposure to the perturbing field in the V_{chan} case. The principle of superposition for linear, time-invariant, additive processes is not reflected in the results of the present experiment. We therefore conclude that movement error estimates derived from vision and proprioception need not be represented in a common coordinate frame for adaptive trajectory regulation. These findings contrast with previous experimental results suggesting additive sensory integration in static limb positioning tasks (van Beers et al. 1996) object discrimination (Ernst and Banks 2002) and movement planning (Sober and Sabes 2003). Although our results clearly indicate that the suppression of visual errors reduces or eliminates the correction of direction errors, it does not appear to eliminate

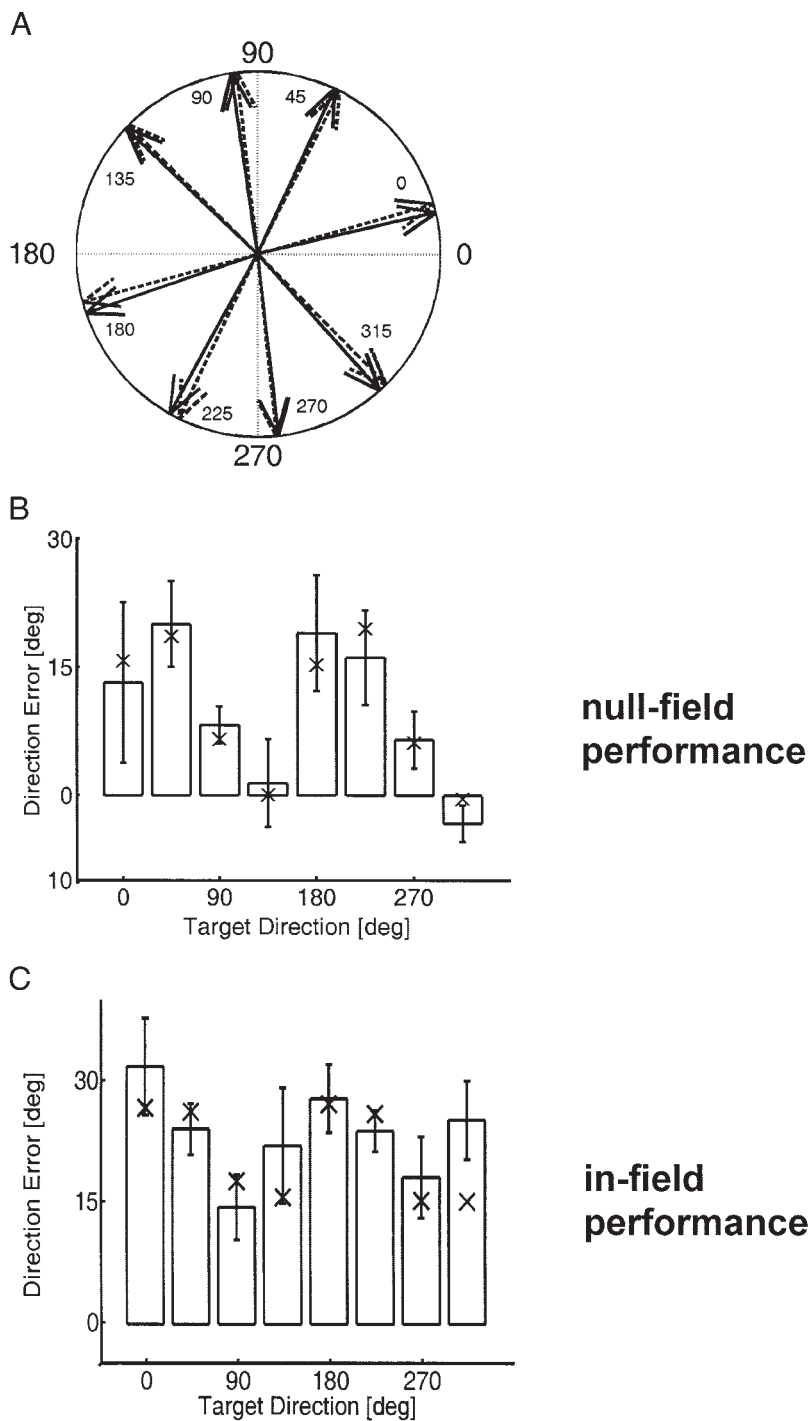


FIG. 7. Comparison of results from numerical simulations and average subject null-field performance in the final V_{chan} adaptation block. *A*: unit vector representation of initial movement directions for catch trials movements toward each of 8 different target directions. Solid arrows correspond to mean initial direction errors calculated across subjects for the target direction (degrees) indicated adjacent to each vector. Dashed arrows correspond to model predictions of initial direction errors consequent to misestimation of initial limb configuration as described in the text. *B*: hand-path direction errors in catch trials without an additional force-field perturbation (calculated by subtracting the intended target angle value from the angle presented in *A*). In this and the following panel, error bars represent 95% CI of the mean across all 5 subjects. \times , indicate the simulated direction errors predicted when motor commands for “ideal” reaching movements from one starting hand position are applied to the same limb, but starting at another, different initial hand position (the hand displaced 6.8 cm toward the subject’s midline and 13.6 cm toward the subject’s chest). *C*: hand-path direction errors in trials with the viscous curl force-field perturbation. The unmodified (unadapted) motor commands used to simulate movements summarized in *A* and *B* were also used to generate the simulated, perturbed movements indicated by the \times , after translating the limb’s initial configuration as described for *B*.

adaptive changes altogether. For example (Fig. 5), corrective submovements induced by the disturbance are progressively suppressed by repeated practice in all feedback conditions. In the presence of correct visual feedback (or in its complete absence), the smoothing of the hand trajectory results in the recovery of the unperturbed kinematics. However, when the visual errors are suppressed by false feedback, the same tendency to smoother motions leads to a modified trajectory, with large direction errors and final errors that are not necessarily in the direction of the disturbing forces. We conclude from these observations and from simulation studies that vision and proprioception may either

compete in the shaping of trajectories or they can have a dominant effect in different phases of movement (e.g., initiation, termination). What appears to be excluded by our findings is the view that these different sensory channels operate through a mechanism of superposition in which each sensory modality plays a relatively fixed role.

Role of proprioception in planning and regulation of hand trajectories

Several studies of sensor fusion for perception of limb state have modeled sensory integration using a weighted summation

of visual and proprioceptive information (e.g., Gharamani et al. 1997; Rossetti et al. 1995; Tardy-Gervet et al. 1986; van Beers et al. 1996, 1999). For example, Sober and Sabes (2003) recently inferred differences in the way vision and proprioception contribute to the planning of reaching movements. By analyzing hand-path errors resulting from manipulations of the hand's initial position and cursor feedback of that position, Sober and Sabes (2003) constructed a linearly weighted model for the sensory integration processes supporting movement vector selection (deciding the direction in which to move the hand) and motor command specification (computing the joint torques required to move along the desired vector). Movement vector selection was estimated to be driven almost exclusively by visual evaluation of initial limb configuration, whereas motor command formulation was estimated to be driven primarily by proprioception (66%), with weaker contribution from vision (34%). Implicit to this argument is the assumption that the nervous system transforms hand position and target location into a common coordinate frame prior to selecting (and programming) a desired movement vector. It is impossible to determine with the current data set whether the force-field adaptations observed in VP and P feedback conditions resulted from weighted combination of visual and proprioceptive estimates of hand-path errors as in the model of Sober and Sabes (2003). It is, however, quite clear that a linear combination cannot adequately describe subject performance in the V_{chan} case.

A recent study has explored the consequence of manipulating the "reliability" of visual feedback during reaching and has elaborated an elegant computational basis for context-dependent adjustments to motor performance (Kording and Wolpert 2003). The investigators asked subjects to reach within a virtual reality environment that could displace visual feedback of hand position relative to the hands actual position by an amount that varied randomly from one trial to the next, drawn from one of two prior distributions—Gaussian and bimodal. The reliability of sensory feedback was also varied by blurring the visual feedback of finger position that was presented briefly half-way through the movement. After extensive training in the task, subjects combined prior knowledge of the distribution with sensory evidence provided during movement to generate compensatory corrections later in the movement. The less reliable the visual information, the more subjects relied on prior knowledge of displacement statistics (the subject's *expectation* of the upcoming displacement) to adjust movement. The authors explain their results within the framework of bayesian optimal estimation theory wherein adjustments to ongoing motor commands are dependent on both the reliability of sensory feedback and on an estimation of prior probabilities of perturbation (i.e., the task *context* within which subjects are asked to perform). They conclude by proposing that bayesian processes might be fundamental to all aspects of sensorimotor control and learning.

As developed by Kording and Wolpert (2003), the bayesian theory does not address how visual and proprioceptive information might jointly contribute to a subject's assessment of sensory reliability and thus the extent to which motor performance might be influenced by expectations of perturbation (i.e., prior probabilities). Because the visual and proprioceptive sensory organs encode position information in different coordinate frames (cf. Soechting and Flanders 1989; Tillery et al.

1991), there will always be "disagreement" between visual and proprioceptive feedback of limb position and movement. Proprioceptors inherently encode muscle length and rate of length change (cf. Cordo et al. 1994; Matthews 1963) while vision encodes object location in egocentric coordinates. Thus it is not clear how the "reliability" of sensory information may be impacted when the usual mapping between proprioceptive and visual estimates of limb position is altered such that many hand positions map onto a single cursor location as in our V_{chan} condition. Our results indicate that reducing variation in visual error estimates eliminates adaptive correction of direction errors but does not eliminate adaptive changes to terminal features of movement consistent with a reduction in secondary corrective movements. Consequently, it seems unlikely that the differential effect of the visual channel on initial movement direction and terminal movement smoothness can be explained by a single, context-based alteration in sensory weighting. Rather our data support the idea that there may be different mechanisms for adapting the initial and final components of movement—a trajectory controller and a postural controller (cf. Brown et al. 2003). Under this hypothesis, we show that vision contributes most predominantly to the regulation of hand-path direction and extent (see also Sober and Sabes 2003), whereas proprioception plays an important role in bringing the hand smoothly to rest at the final hand location or limb posture.

Evolution of initial direction errors

An explanation for the progressively increasing direction errors observed in the V_{chan} case derives from empirical observations that proprioceptive estimates of static limb position tend to drift over time when active limb movement and ongoing visual feedback of the hand or limb are prevented (Wann and Ibrahim 1993). Drifts are toward the subject's midline or more frequently used workspace (Ghez et al. 1999) and are thought to arise because proprioceptive maps relating limb configuration to the hand's position in extrinsic space require constant visual updating or "recalibration" (Ghilardi et al. 1995; Rossetti et al. 1995; Wann and Ibrahim 1993). The degradation of proprioceptive maps can be arrested by showing a visual representation of the hand's true position between movements (as in our P condition). In one of the clearest demonstrations of "drift," Brown et al. (2003) asked subjects to perform many reaching movements out-and-back between targets in the horizontal plane without ongoing visual feedback of hand location. Over ~ 70 trials, the start location of each movement drifted away from the initial start location by 8 cm toward the subject's midsagittal plane. Movement distance and direction remained relatively constant despite this drift. These authors performed forward dynamic simulations showing that preservation of movement distance and direction required subjects to adjust their motor commands to account accurately for changes in initial limb configuration. Failure to do so would generate movements with considerable direction errors. Consequently, they conclude that proprioception continues to be a reliable source of limb position information, even after prolonged time without vision.

Whereas the study by Brown et al. (2003) allowed subjects to adjust their initial hand location from trial to trial, our subjects were forced to start their movements from a single

starting location. Thus we were precluded from observing an accumulation of errors in the starting location of movements. Rather, we observed an accumulation of movement direction errors in our V_{chan} condition that we reasoned result from erroneous estimates of initial hand position, even though regularity of initial limb configuration was enforced. We performed a set of forward dynamic simulations to evaluate whether erroneous estimates of initial hand position could in fact give rise to the pattern of hand-path errors made after repeated exposure to the force field. We made the assumption that subjects did not adapt motor commands to the force field during the initial phase of movement because they did not exhibit clear adaptation of initial direction under V_{chan} feedback in either *protocol P1* or *P3* (no adaptation in the null field of *P2* was expected). Our simulations demonstrated that initial limb configuration estimation errors do account for the direction errors made toward most targets. The same limb configuration errors used to predict initial direction errors in movements to seven of eight targets within the null field (catch trials) also sufficed to predict initial direction error in the viscous curl field of *P1*. Progressively increasing direction errors can be explained concisely by only two parameters (i.e., progressively increasing errors in either initial hand position or, equivalently, joint angle estimates).

The conclusion drawn by Brown et al. (2003)—namely, that proprioception continues to be a reliable source of limb position information in the absence of visual feedback—appears to conflict with our observation that subjects gradually develop movement direction errors consistent with erroneous estimates of initial hand position, even though they are provided with truthful information about initial hand position in extrinsic space. How can proprioception provide accurate estimates of initial limb configuration when the hand is free to drift (cf. Brown et al. 2003), whereas proprioceptive estimates of initial limb configuration appear to drift when hand position is constrained?

Instead of regarding proprioceptive estimates of limb position as requiring calibration to a visual coordinate frame, it may be more appropriate to consider the mapping of visually specified target locations into “desired” limb configurations as ephemeral because visual information for specifying movement objectives has a limited useful lifetime and must necessarily adjust with head and eye movements (Goodale and Milner 1992; Goodale et al. 1994). Accumulation of errors in the transformation from a visual target location to a desired limb configuration would give rise to the observation of a real drift in initial hand location if these errors equally influenced both the starting and final target representations used to calculate the desired movement vector (Sober and Sabes 2003). In this case, the visually specified targets would map into (erroneous) initial and final “desired” limb configurations, which the subject would use to select and program reaching movements. Furthermore, movement distance and direction would be preserved as in Brown et al. (2003) because the equal accumulation of errors across target locations represents a simple translation between the visual and proprioceptive maps of the limb’s workspace. When proprioceptive and (erroneous) visual estimates of initial limb position coincide at the “shifted” location, computed torques based from that position should still yield movements that are appropriately directed with proper extent.

But when the hand is constrained to start from a single location as in the present study, drift in the mapping between visual target locations and “desired” initial and final limb configurations would lead to a gradual divergence of robotically enforced and visually estimated initial conditions. If the initial limb position estimate used to program the desired reach is a weighted combination of an (erroneous) visual estimate of the desired initial limb configuration and an accurate proprioceptive estimate of the limb’s actual position, (cf. Sober and Sabes 2003), then the computed torques would not be appropriate for the hand’s enforced start position but rather for a position located between the accurate proprioceptive estimate and the inaccurate visual estimate. The consequence of these motor programming errors are demonstrated by our simulations and are consistent with the errors generated by all of our subjects. We therefore conclude that selective visual feedback of hand-path errors *along* the desired direction of movement is ineffectual in calibrating the mapping between start target location and desired initial limb configuration.

Separation of trajectory and final position control?

An important experimental finding has been that in the visual channel subjects persist in generating large deviations between target and final hand position (Fig. 2) even while trajectory smoothness is recovered with practice. This has not been previously observed during adaptation to velocity-dependent force fields within a single limb, although a similar separation of endpoint and trajectory adaptation has been observed in the inter-limb transfer of adaptation to Coriolis forces (Dizio and Lackner 1995). At least two different models may account for this finding. One possibility is that trajectory regulation and final position regulation are mediated by two different control mechanisms (Dizio and Lackner 1995; Hirayama et al. 1993; Kawato 1991; Sainburg et al. 1999; see also Ghez 1979; Massion 1992). The first operates in a feed forward manner and regulates trajectory execution while the second regulates final limb posture and is strongly influenced by ongoing visual feedback. Accordingly, the control of reaching movements may be partitioned into a transport phase concerned with enforcing rectilinear motion and a stabilization phase concerned with reducing unnecessary motion of the hand about its desired final position. An alternative hypothesis is that, in the absence of visual feedback of errors, the motor system drastically reduces the stiffness about the desired trajectory. In this case, the final errors, which are in the direction of the forces experienced during movement, could be accounted for by minimal level of friction in the experimental apparatus. The determination of which factors contribute to final position error will require additional investigation.

APPENDIX

We performed a set of numerical simulations to evaluate the consequence of mis-estimating initial limb posture on the subsequent generation of reaching movements. The arm was modeled as a two-segment link in the horizontal plane (Fig. 1C). Each segment is modeled as a homogeneous rigid body with mass m concentrated at the center of mass located at distance r from the proximal joint. Each segment i also has a moment of inertia I_i where the index $i = s$

corresponds to the shoulder joint, whereas $i = e$ corresponds to the elbow joint.

Ideal, straight-line, template movements of 12.0 cm length (e.g., Fig. 1C) and bell-shaped hand-speed profiles (Fig. 1D) were created within the MATLAB computing environment (ver. 6.1.0.450, The Mathworks, Natick, MA). These template movements originated from a central position 0.4 m in front of the shoulder, with the 90 and 180° movements aligned with the axis passing through the shoulder.

The anthropometric parameters used for simulating a “typical subject” were taken from previously published simulations of reaching and adaptation to velocity-dependent force fields (Table A1) (Shadmehr and Mussa-Ivaldi 1994). Inverse kinematics calculations were performed to calculate the shoulder and elbow joint angle excursions required to perform each of the template movements. The shoulder and elbow joint torques required to drive the simulated limb through the template trajectories were calculated using inverse dynamic equations of motion (Eq. A1)

$$\begin{bmatrix} \tau_s \\ \tau_e \end{bmatrix} = \begin{bmatrix} I_s + I_e + m_s r_s^2 + m_e r_e^2 + I_e^2 m_e + 2I_s m_e r_e \cos(\theta_e) & I_e + m_e r_e^2 + I_s m_e r_e \cos(\theta_e) \\ I_e + m_e r_e^2 + I_s m_e r_e \cos(\theta_e) & I_e + m_e r_e^2 \end{bmatrix} \begin{bmatrix} \ddot{\theta}_s \\ \ddot{\theta}_e \end{bmatrix} \\ + \begin{bmatrix} 0 & -I_s m_e r_e \sin(\theta_e) & -2I_s m_e r_e \sin(\theta_e) \\ I_s m_e r_e \sin(\theta_e) & 0 & 0 \end{bmatrix} \begin{bmatrix} \dot{\theta}_s \\ \dot{\theta}_e \end{bmatrix} + \begin{bmatrix} V_{11} & V_{12} \\ V_{21} & V_{22} \end{bmatrix} \begin{bmatrix} \dot{\theta}_s - \dot{\theta}_{s_template} \\ \dot{\theta}_e - \dot{\theta}_{e_template} \end{bmatrix} + \begin{bmatrix} K_{11} & K_{12} \\ K_{21} & K_{22} \end{bmatrix} \begin{bmatrix} \theta_s - \theta_{s_template} \\ \theta_e - \theta_{e_template} \end{bmatrix} \quad (A1)$$

Note that terms depending on the \mathbf{V} and \mathbf{K} matrices do not contribute to the torques calculated along the template movements because the difference terms $(\theta_i - \theta_{i_template})$ and $(\dot{\theta}_i - \dot{\theta}_{i_template})$ are, by definition, zero along the templates. The calculated torques, therefore are strictly feedforward in nature. Note also that $\theta_{i_template}$ and $\dot{\theta}_{i_template}$ are functions of time and are specified in term of joint displacements relative to an initial joint configuration. Thus altering the initial limb configuration will induce an effective perturbation to motion (by altering reaction torques and the effective inertia of the limb) that will be opposed by position- and velocity-dependent restoring forces dependent on $\theta_{i_template}$ and $\dot{\theta}_{i_template}$. So, given a shift in the limb's initial configuration, forward dynamic equations of motion (i.e., the inverse of Eq. A1) were propagated forward in time subject to the feedforward torques calculated along the template movements as well as the ideal joint displacements $\theta_{i_template}$ and $\dot{\theta}_{i_template}$.

Finally, the simplex approach to multi-dimensional, nonlinear optimization (Press et al. 1988) was used to choose shoulder and elbow initial condition displacements that would minimize the weighted difference between two vectors. The first vector, α , was comprised of an ordered list of direction and extent errors averaged across subjects (i.e., the mean error values presented in Fig. 3, A and B). The second vector, β , was similar, except it was composed of direction and extent errors predicted by our numerical simulation. The optimization minimized the cost function ϕ (Eq. A2)

$$\phi = \sum_{i=1}^N k_i (\alpha_i - \beta_i)^2 \quad (A2)$$

where $N = 16$, the number of elements in each of the two error vectors. The scaling factors k_i were selected so that directional and extent errors contributed about equally to the cost function ϕ , thus ensuring that the optimization was not inappropriately biased toward minimizing either errors in direction or errors in extent. The simulation results reported in the text were robust to changes in scaling factors k_i .

TABLE A1. Anthropometric and joint mechanical property values used in numerical simulations of reaching movements as described in the text

Parameter	Value
Upper arm length, m	0.33
Upper arm mass, kg	1.93
Upper arm COM, m	0.165
Upper arm inertia, kg/m ²	0.0141
Forearm/hand length, m	0.34
Forearm/hand mass, kg	1.52
Forearm/hand COM, m	0.19
Forearm/hand inertia, kg/m ²	0.0188
Joint stiffness matrix	$K = \begin{bmatrix} -15 & -6 \\ -6 & -16 \end{bmatrix}$ N/rad
Joint damping matrix	$V = \begin{bmatrix} -2.3 & -0.9 \\ -0.9 & -2.4 \end{bmatrix}$ Ns/rad

COM, center of mass.

ACKNOWLEDGMENTS

We thank Dr. Claude Ghez for insightful comments regarding an early draft of this manuscript.

GRANTS

This work was supported by Whitaker Foundation Grant RG010157, National Science Foundation Grant 0238442, National Institute of Neurological Disorders and Stroke Grant 2R01NS-35673 and by grants from Ministero dell' Istruzione, dell' Università e della Ricerca and the Alvin W. and Marion Birnschein Foundation.

REFERENCES

- Atkeson CG and Hollerbach JM.** Kinematic features of unrestrained vertical arm movements. *J Neurosci* 5: 2318–2330, 1985.
- Bock O and Arnold K.** Error accumulation and error correction in sequential pointing movements. *Exp Brain Res* 95: 111–117, 1993.
- Brown LE, Rosenbaum DA, and Sainburg RL.** Limb position drift: implications for control of posture and movement. *J Neurophysiol* 90: 3105–3118, 2003.
- Conditt M.** *Central Mechanisms for Adaptation of Multi-Joint Arm Movements.* Evanston, IL: Northwestern University, 1998.
- Conditt MA, Gandolfo F, and Mussa-Ivaldi FA.** The motor system does not learn the dynamics of the arm by rote memorization of past experience. *J Neurophysiol* 78: 554–560, 1997a.
- Conditt MA, Scheidt RA, and Mussa-Ivaldi FA.** Visual influence on learning arm dynamics. *Soc Neurosci Abstr* 23: 36, 1997b.
- Cordo P, Carlton L, Bevan L, Carlton M, and Kerr GK.** Proprioceptive coordination of movement sequences: role of velocity and position information. *J Neurophysiol* 71: 1848–1861, 1994.
- Desmurget M, Pelisson D, Rossetti Y, and Prablanc C.** From eye to hand: planning goal-directed movements. *Neurosci Behav Rev* 22: 761–788, 1998.
- Desmurget M, Rossetti Y, Jordan M, Meckler C, and Prablanc C.** Viewing the hand prior to movement improves accuracy of pointing performed toward the unseen contralesional hand. *Exp Brain Res* 115: 180–186, 1997.
- Desmurget M, Vindras P, Grea H, Viviani P, and Grafton ST.** Proprioception does not quickly drift during visual occlusion. *Exp Brain Res* 134: 363–377, 2000.
- Dizio P and Lackner JR.** Motor adaptation to Coriolis force perturbations of reaching movements: endpoint but not trajectory adaptation transfers to the non-exposed arm. *J Neurophysiol* 74: 1787–1792, 1995.

- Dizio P and Lackner JR.** Congenitally blind individuals rapidly adapt to Coriolis force perturbations of their reaching movements. *J Neurophysiol* 84: 2175–2180, 2000.
- Ernst MO and Banks MS.** Humans integrate visual and haptic information in a statistically optimal fashion. *Nature* 415: 429–433, 2002.
- Flanagan JR and Rao AK.** Trajectory adaptation to a nonlinear visuomotor transformation: evidence of motion planning in visually perceived space. *J Neurophysiol* 74: 2174–2178, 1995.
- Flanders M, Helms-Tillery SI, and Soechting JF.** Early stages in a sensorimotor transformation. *Behav Brain Sci* 15: 309–362, 1992.
- Gharamani Z, Wolpert DM, and Jordan MI.** Computational models of sensorimotor integration. In: *Self-Organization, Computational Maps and Motor Control*, edited by Morasso PG and Sanguineti V. Amsterdam: North-Holland, 1997, p. 117–147.
- Ghez C.** Contributions of central programs to rapid limb movement in the cat. In: *Integration in the Nervous System*, edited by Asanuma H and Wilson VJ. Tokyo, Japan: Igaku-Shoin, 1979, p. 305–319.
- Ghez C, Gordon J, and Ghilardi MF.** Programming of extent and direction in human reaching movements. *Biomed Res* 14: 1–5, 1993.
- Ghez C, Gordon J, and Ghilardi MF.** Impairments of reaching movements in patients without proprioception. II. Effects of visual information on accuracy. *J Neurophysiol* 73: 361–372, 1995.
- Ghez C, Krakauer JW, Sainburg RL, and Ghilardi M-F.** Spatial representations and internal models of limb dynamics in motor learning. In: *The New Cognitive Neurosciences* (2nd ed.), edited by Gazzaniga MS. Cambridge, MA: The MIT Press, 1999, p. 501–514.
- Ghilardi MF, Gordon J, and Ghez C.** Learning a visuomotor transformation in a local area of workspace produces directional biases in other areas. *J Neurophysiol* 73: 2535–2539, 1995.
- Goodale MA and Milner AD.** Separate visual pathways for perception and action. *Trends Neurosci* 15: 20–25, 1992.
- Goodale MA, Jakobson LS, and Keillor JM.** Differences in the visual control of pantomimed and natural grasping movements. *Neuropsychologia* 32: 1159–1178, 1994.
- Gordon J, Ghilardi MF, and Ghez C.** Accuracy of planar reaching movements. I. Independence of direction and extent variability. *Exp Brain Res* 99: 97–111, 1994.
- Graziano MS.** Where is my arm? The relative role of vision and proprioception in the neuronal representation of limb position. *Proc Natl Acad Sci USA* 96: 10418–10421, 1999.
- Graziano MS, Cooke DF, and Taylor CS.** Coding the location of the arm by sight. *Science* 290: 1782–6, 2000.
- Hirayama M, Kawato M, and Jordan MI.** The cascade neural network model and a speed-accuracy trade off of arm. *J Mot Behav* 25: 162–174, 1993.
- Kawato M.** Optimization and learning in neural networks for formation and control of coordinated movement. In: *Attention and Performance XIV*, edited by Meyer D. Hillsdale, NJ: Erlbaum, 1991.
- Krakauer JW, Ghilardi MF, and Ghez C.** Independent learning of internal models for kinematic and dynamic control of reaching. *Nat Neurosci* 2: 1026–1031, 1999.
- Kording KP and Wolpert DM.** Bayesian integration in sensorimotor learning. *Nature* 427: 244–247, 2003.
- Lackner JR and Dizio P.** Rapid adaptation to coriolis force perturbations of arm trajectory. *J Neurophysiol* 72: 299–313, 1994.
- Lagarias JC, Reeds JA, Wright MH, and Wright PE.** Convergence properties of the Nelder-Mead simplex method in low dimensions. *SIAM J Optimizat* 9: 112–147, 1998.
- Massion J.** Movement, posture and equilibrium: interaction and coordination. *Prog Neurobiol* 38: 35–56, 1992.
- Matthews PBC.** The response of de-efferented muscle spindle receptors to stretching at different velocities. *J Physiol* 168: 660–678, 1963.
- McDonough RN and Whalen AD.** *Detection of Signals in Noise*. San Diego, CA: Academic, 1995.
- Meyer DE, Abrams RA, Kornblum S, Wright CE, and Smith JEK.** Optimality in human motor performance: ideal control of rapid aimed movements. *Psychol Rev* 95: 340–370, 1988.
- Morasso P.** Spatial control of arm movements. *Exp Brain Res* 42: 223–227, 1981.
- Press WH, Flannery BP, Teukolsky SA, and Vetterling WT.** *Numerical Recipes in C; the Art of Scientific Computing*. Cambridge, UK: Cambridge Univ. Press, 1988.
- Prochazka A.** Proprioceptive feedback and movement regulation. In: *Handbook of Physiology. Am J Physiol Exercise*. New York: Oxford, 1996, sect. 12, p. 89–127.
- Rosenbaum DA.** Human movement initiation: specification of arm, direction, and extent. *J Exp Psych* 109: 444–474, 1980.
- Rossetti Y, Desmurget M, and Prablanc C.** Vectorial coding of movement: vision, proprioception, or both? *J Neurophysiol* 74: 457–463, 1995.
- Sainburg RL, Ghez C, and Kalkanis D.** Intersegmental dynamics are controlled by sequential anticipatory error correction and postural mechanisms. *J Neurophysiol* 81: 1045–1056, 1999.
- Sainburg RL, Ghilardi MF, Poizner H, and Ghez C.** Control of limb dynamics in normal subjects and patients without proprioception. *J Neurophysiol* 73: 820–835, 1995.
- Sainburg RL, Lateiner JE, Latash ML, and Bagesteiro LB.** Effects of altering initial position on movement direction and extent. *J Neurophysiol* 89: 401–415, 2003.
- Scheidt RA, Dingwell J, and Mussa-Ivaldi FA.** Learning to move amid uncertainty. *J Neurophysiol* 86: 971–985, 2001.
- Schreiner RC, Essick GK, and Whitsel BL.** Variability in somatosensory cortical neuron discharge: effects on capacity to signal different stimulus conditions using a mean rate code. *J Neurophysiol* 71: 338–349, 1978.
- Secco EL, Scheidt RA, Patton J, and Mussa-Ivaldi FA.** Misrepresentation of limb dynamics induced by the suppression of visual errors. *Soc Neurosci Abstr* 29, 2003.
- Shadmehr R and Mussa-Ivaldi FA.** Adaptive representation of dynamics during learning of a motor task. *J Neurosci* 14: 3208–3224, 1994.
- Sober SJ and Sabes PN.** Multisensory integration during motor planning. *J Neurosci* 23: 6982–6992, 2003.
- Soechting JF and Flanders M.** Sensorimotor representations for pointing to targets in three-dimensional space. *J Neurophysiol* 62: 582–594, 1989.
- Tardy-Gervet M-F, Gilhodes J-C, and Roll J-P.** Interactions between visual and muscular information in illusions of limb movement. *Behav Brain Res* 20: 161–174, 1986.
- Thoroughman KA and Shadmehr R.** Learning of action through adaptive combination of motor primitives. *Nature* 407: 742–746, 2000.
- Tillery SI, Flanders M, and Soechting JF.** A coordinate system for the synthesis of visual and kinesthetic information. *J Neurophysiol* 11: 770–778, 1991.
- Tong C, Wolpert DM, and Flanagan JR.** Kinematics and dynamics are not represented independently in motor working memory: evidence from an interference study. *J Neurosci* 22: 1108–13, 2002.
- van Beers RJ, Baraduc P, and Wolpert DM.** Role of uncertainty in sensorimotor control. *Phil Trans R Soc Lond B Biol Sci* 357: 1137–1145, 2002.
- van Beers RJ, Sittig AC, and Gon JJDvd.** How humans combine simultaneous proprioceptive and visual position information. *Exp Brain Res* 111: 253–261, 1996.
- van Beers RJ, Sittig AC, and Gon JJDvd.** Integration of proprioceptive and visual position-information: an experimentally supported model. *J Neurophysiol* 81: 1355–1364, 1999.
- Vindras P, Desmurget M, Prablanc C, and Viviani P.** Pointing errors reflect biases in the perception of the initial hand position. *J Neurophysiol* 79: 3290–3294, 1998.
- Wann JP and Ibrahim SF.** Does limb proprioception drift? *Exp Brain Res* 91: 162–166, 1993.
- Whitsel BL, Schreiner RD, and Essick GK.** An analysis of variability in somatosensory cortical neuron discharge. *J Neurophysiol* 40: 589–607, 1977.
- Wolpert DM, Gharamani Z, and Jordan MI.** Perceptual distortion contributes to the curvature of human reaching movements. *Exp Brain Res* 98: 153–156, 1994.
- Wolpert DM, Gharamani Z, and Jordan MI.** Are arm trajectories planned in kinematic or dynamic coordinates? An adaptation study. *Exp Brain Res* 103: 460–470, 1995.
- Ziemer RE, Tranter WH, and Fannin DR.** *Signals and Systems: Continuous and Discrete*. New York: Macmillan, 1983.